

Ions-Induced Nanostructuration: Effect of Specific Ionic Adsorption on Hydrophobic Polymer Surfaces

Igor Siretanu,^{†,‡,¶} Jean-Paul Chapel,^{†,‡} Delfi Bastos-González,[§] and Carlos Drummond^{*,†,‡}

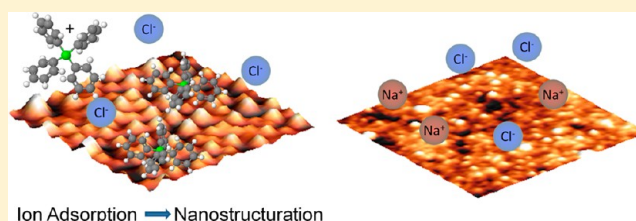
[†]CNRS, Centre de Recherche Paul Pascal (CRPP), UPR 8641, F-33600 Pessac, France

[‡]Université Bordeaux 1, CRPP, F-33600 Pessac, France

[§]Biocolloid and Fluid Physics Group, Department of Applied Physics, University of Granada, Av. Fuentenueva S/N, 18071 Granada, Spain

Supporting Information

ABSTRACT: The effect of surface charges on the ionic distribution in close proximity to an interface has been extensively studied. On the contrary, the influence of ions (from dissolved salts) on deformable interfaces has been barely investigated. Ions can adsorb from aqueous solutions on hydrophobic surfaces, generating forces that can induce long-lasting deformation of glassy polymer films, a process called ion-induced polymer nanostructuration, IPN. We have found that this process is ion-specific; larger surface modifications are observed in the presence of water ions and hydrophobic and amphiphilic ions. Surface structuration is also observed in the presence of certain salts of lithium. We have used streaming potential and atomic force microscopy to study the effect of dissolved ions on the surface properties of polystyrene films, finding a good correlation between ionic adsorption and IPN. Our results also suggest that the presence of strongly hydrated lithium promotes the interaction of anions with polystyrene surfaces and more generally with hydrophobic polymer surfaces, triggering then the IPN process.



■ INTRODUCTION

The importance of understanding the behavior of electrically charged surfaces in contact with ionic solutions in many biological and industrial problems can hardly be overestimated. First, the cause of the electric charge must be examined. The interface between the two initially electroneutral phases (surface and solution) can become electrically charged by a number of different processes: ionization of functional groups, preferential adsorption of ions or desorption, or exchange of lattice ions. Then, a number of variables have to be inspected to characterize the surface, the media, and the boundary conditions. A satisfactory description of this problem at low salt concentrations can be achieved by mean field theories, developed after the work of Gouy and Chapman, which is the starting point for the celebrated Poisson–Boltzmann equation.¹ However, it is well documented that this description often fails at moderate to high salt concentrations. One aspect that cannot be accounted for by this simple description is the distinct effect of particular ions, because this approach only considers the ionic charge and does not take into account the discrete nature of ions or solvent molecules, or the possibility of correlation between the charges. The error introduced by considering ions as indistinct point charges, neglecting the dispersion forces involving the ions and their disruptive effect on the solvent, becomes unacceptable as ionic strength increases. Another source of error that is frequently overlooked is related to the deformability of the boundary. Frequently, only the influence of surface charges on the ionic distribution in the liquid phase is

investigated. On the contrary, the possible effect of the ionic distribution on the surface itself is frequently ignored: the walls are often considered to be unalterable and nondeformable. This assumption is adequate for hard solid walls, but is certainly not so for soft boundaries, e.g., charged membranes or polymer substrates. For instance, we have recently reported that smooth, hydrophobic surfaces of a glassy polymer can be substantially deformed due to the effect of water ions: we put forward the idea that the ion-induced electrostatic field induces long-lasting deformations of the hydrophobic wall.² We have called this phenomenon ion-induced polymer nanostructuration, IPN. As we have described in the past, the typical size of the self-assembled patterns depends on pH, temperature, and the amount of dissolved gas in the aqueous phase, as well as on the mobility of the surface, which can be affected by the interaction with the supporting substrate.³

For the case of deformable interfaces the interplay between the electrostatic problem, determined by the charge distribution, and the boundary shape, governed by hydrodynamic and mechanic considerations, is an extremely involved problem. The wall shape and the electrostatic boundary conditions are intermingled and cannot be treated independently: the presence of the ions distort the shape of the surface, changing the boundary conditions of the electrostatic problem that

Received: January 16, 2013

Revised: March 24, 2013

Published: May 7, 2013

determines the ionic distribution itself. The experimental study of this problem is also complicated, as the charge-induced surface modifications are typically short-lived and difficult to observe without perturbing the system. This is not true for the case of deformed glassy polymer surfaces mentioned above: if the temperature is lower than the glass transition temperature of the polymer, relaxation of the ion-induced perturbation takes a long time; the deformed surface can then be studied *ex situ*. Thus, a complete study of the effect of different variables involved in the problem can be performed, which is out of reach for quickly relaxing boundaries (e.g., soft membranes or rubbery polymers). In this work, we investigated the influence of different salts on IPN and we found that the effect is ion-specific. By combining atomic force microscopy in tapping and force modes and streaming potential measurements, we show that the deformation of the hydrophobic wall is correlated with the surface charge produced by ionic adsorption on the polymer–water interface.

MATERIALS AND METHODS

Film Preparation. The polystyrene PS films were prepared by spin coating solutions of the polymer (250 kg/mol, ACROS Organics) in toluene 5% w/w onto silicon wafers. The wafers were previously cleaned with Piranha solution during 1 h to remove dust and organic contaminants (Caution! Piranha is a strong oxidant and reacts violently with organic substances). Then, the surfaces were extensively rinsed with Millipore water and gently dried with N_2 gas. Because the piranha mixture is a strong oxidizer, it removes most organic matter, and hydroxylates the Si surface (adding OH groups), making it extremely hydrophilic. The oxide layer on top of the silicon substrates was around 2 nm thick after piranha treatment. To increase the adhesion of the polymer film on the substrates and to avoid the penetration of water underneath the films, the silicon wafers were coated with a silane layer by 2 h exposure to a solution of octadecyltrimethoxysilane, OTS (abcr Specialty Chemicals) in toluene before spin coating. The cast PS films were annealed at 95 °C for 12 h to remove the residual solvent and release any mechanical stress built up during the spin-coating process.

Water Degassing and Film Treatment. Millipore water with resistivity of 18 M Ω ·cm was used for preparation of all solutions investigated. Carefully cleaned Teflon bar stirrers were introduced in the solution to be degassed to induce the nucleation of gas bubbles. The solutions were subjected to mild agitation under pressure of 0.2 mbar during 2 h (formation of macroscopic bubbles in the aqueous phase was typically observed only during the first 30 min of degassing). Then the air pressure on the flask was gently increased back to atmospheric pressure, and the solutions were put right away in contact with the polymer surfaces for a few minutes. Similar results were observed after longer exposure times. The treated PS films were then dried with a gentle flow of nitrogen gas.

For studying different pH conditions, the pH of the (unbuffered) aqueous phase was adjusted by adding small amounts of NaOH (Prolabo), KOH (Aldrich), HCl (Aldrich), or nitric acid (Aldrich) as necessary. LiF, LiBr, KCl, KI, NaCl, NaNO₃, NaI, NH₄Cl, HCl, N(*n*-butyl)₄Cl, N(*n*-butyl)₄I, N(*n*-butyl)₄NO₃, sodium tetraphenylborate (Ph₄BNa), and tetraphenylarsonium chloride (Ph₄AsCl) were obtained from Aldrich; LiNO₃ was purchased from Scharlau; LiCl, NaBr, N(*n*-butyl)₄Br, N(ethyl)₄I, N(methyl)₄I, DTAB, and SDS were obtained from Fluka; NaClO₄, K₂SO₄, and NaCH₃COO were

obtained from Acros. LiI, NH₄NO₃, CsI, and LiSO₄ were purchased from Prolabo. All the salts were of the highest quality available and were used as received. Salt concentrations of 0.03 M were used, unless otherwise indicated.

Film Characterization. Roughness and morphology of the PS films before and after treatment with ionic solutions were assessed by atomic force microscopy in tapping mode (NanoScope III Multimode, Veeco, and Icon, Bruker) using Si tips on rectangular Si cantilevers. Extremely smooth films of thickness 300 nm with a rms roughness smaller than 0.5 nm (measured on 1 × 1 μ m² images) were typically obtained after spin coating. The contact angle of water on the films was around 90° with very small hysteresis for pH between 1.5 and 11. An important modification of the film morphology was observed upon treatment with certain degassed ionic solutions, as described below.

Atomic Force Microscopy: Force Curves. The solid/electrolyte solution interface was examined using a Veeco NanoScope IVa Multimode atomic force microscope. The solution of interest was held in a standard fluid cell sealed by a silicone O-ring. Both were cleaned by rinsing with ethanol and deionized water and then dried using filtered nitrogen. Force versus separation curves were measured with silicon tip probes on silicon nitride triangular cantilevers 120 μ m long (Bruker). The tips were irradiated with ultraviolet light in an UV/ozone cleaner for 30 min prior to use. A SiO₂ layer forms on the tip surface during this treatment; as the isoelectric point of silica is between pH = 2 and 3, the tips were negatively charged when immersed in water above pH 3.

We measured the interaction between the AFM tip and PS films or freshly cleaved muscovite mica surfaces as a function of the relative tip–substrate distance, in different ionic solutions. The cantilever deflection due to the tip–substrate interaction was determined from the voltage measured on the AFM sectorized photodiode. As customary, we considered the tip to be in contact with the surface when the voltage versus displacement response varied steeply (and linearly): although this is not necessarily true (*vide infra*), we have used this data to calibrate the response of the photodiode for each force curve.⁴ Given that the spring constant is different for each cantilever and the exact geometry of the tip is unknown, we did not attempt to calculate the actual interaction force from the deflection data. However, as we used a single probe for each of the data sets presented, the reported cantilever deflection is an accurate representation of the relative intensity of the force measured for the different systems investigated. The force profiles presented are the result of averaging between 20 and 30 force curves in different spots on the substrates, unless otherwise indicated. It has been reported before that gas nanobubbles may nucleate on hydrophobic surfaces in aqueous environment;^{5,6} indeed, we observe their presence occasionally when imaging the PS substrates by AFM. In a given force curve profile, we interpreted the presence of a soft repulsion between the tip and the substrate during approach, a long-range attractive force with multiple pull-off, steps, or the lack of a single clear snap-off during retraction as being due to nucleated nanobubbles. We have discarded force curves that hint the presence of nanobubbles (about 5% of measured curves).

Compared with other surface force measuring techniques (e.g., the surface forces apparatus), AFM allows performing a relatively easy and quick scan of different environmental conditions. In addition, materials of different nature can be readily explored. However, several limitations have to be

considered when analyzing the data. As mentioned above, the actual geometry of the contact region is not precisely known, although it can be determined a posteriori. More challenging is the fact that the absolute tip–substrate separation cannot be determined. As mentioned, it is often assumed that a steep repulsive force signals tip–substrate contact, which is not necessarily true. This important drawback, often overlooked in the literature, may have important consequences for the analysis of the data, as we will discuss below.

Zeta Potential, ζ . When an electrolyte solution is forced to move across a channel formed by two charged plates by applying a pressure gradient, the excess charges near the wall are carried along by the liquid. Their accumulation downstream causes an electric field to build up, generating a potential difference, the streaming potential, E_s .¹ We measured E_s at different pressure drop values, (ZetaCAD, CAD Instruments). The zeta potential, ζ , was then calculated using the Smoluchowski equation¹

$$\zeta = \frac{E_s \eta k_L}{\epsilon_w \epsilon_0 \Delta p}$$

where ϵ_0 is the electric permittivity of vacuum, and ϵ_w , η , and k_L are the relative permittivity, viscosity, and conductivity of the solution. In this description, nonslip hydrodynamic boundary conditions are assumed. However, it has become clear that partial wall slip is the rule for the case of hydrophobic surfaces in contact with water.^{7,8} A slip-induced amplification of the calculated ζ will then be introduced when this analysis is applied, as described by Bouzigues et al.⁹ It is then important to realize that ζ will include electrostatic and hydrodynamic contributions, which can be separated only if a precise determination of the slip length is possible.

RESULTS AND DISCUSSION

A. Atomic Force Microscope: Surface Morphology Modification. As described in the Introduction, a long-lasting deformation spontaneously appears on smooth polystyrene surfaces after they are put in contact for a few minutes with degassed water solutions (IPN).² As we have reported in the past, a similar effect is observed with other glassy hydrophobic polymers.² Solution degassing is a necessary but not sufficient condition for IPN to occur: as it is shown in this work, no surface deformation is observed without the presence of specific ions in solution. It has been suggested in the past that a region of reduced density may be present at the interface between gas-saturated water and hydrophobic surfaces, although the nature of this depleted layer remains controversial.¹⁰ Degassing the water allows the intimate contact between the two phases. The enhanced proximity between the hydrophobic polymer film and the aqueous solution is at the origin of the spontaneous nanostructuration.

Atomic force microscopy micrographs illustrating this novel phenomenon are presented in Figure 1. It is important to emphasize that these AFM micrographs were measured in air, after the PS substrates were exposed to aqueous solution. The observed nanometric size bumps are not small bubbles nucleated on the surface in contact with water, but the result of the deformation of the polymer surface. The observed deformation is rather mild: at room temperature the self-assembled bumps are typically 5 nm tall and 50 nm large, as can be appreciated in the height profile in Figure 1. We have recently reported that IPN is strongly influenced by the pH of

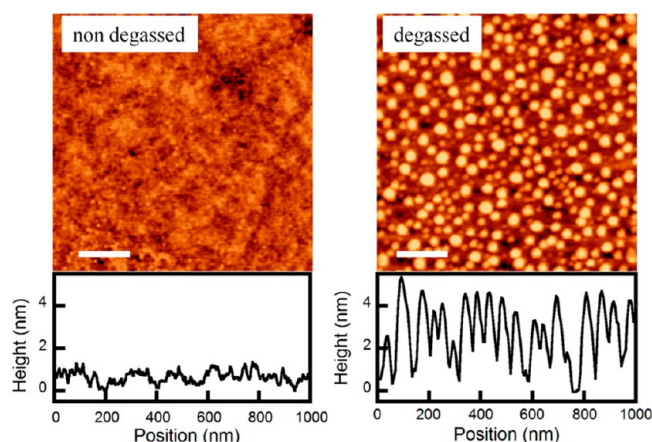


Figure 1. $1 \mu\text{m} \times 1 \mu\text{m}$ height tapping mode AFM micrographs taken in air of 300 nm thick 250 kDa polystyrene films after exposure to nondegassed (left) and degassed (right) solutions of nitric acid in double-distilled water at pH 1.5 and room temperature. A typical height profile for each condition is presented. The presence of asperities of regular nanometric size is clearly observed only on the surface exposed to the degassed solution for 5 min. The scale bars correspond to 200 nm.

the aqueous phase.² In the present work we have performed an extensive study to determine which ions, other than water ions, exert a structuring effect on the PS surfaces, with emphasis on monovalent salts. A compilation of the different salts studied is presented in Table 1. The effect of each salt is recorded at the intersection of the particular cation (rows) and anion (column). Check marks correspond to salts that induced a larger structuration than the one observed for water at similar pH values. The opposite is signaled by crosses. The effect of each salt reported was tested at least three times—with independent surfaces and degassed solutions—to verify reproducibility. We found that the IPN process is ion specific: in many cases, no structuring effect was observed. Several general trends can be inferred from these results.

1. Substantial PS structuration is observed in the presence of water ions ($\text{pH} < 2.5$ or $\text{pH} > 10$). The deformation of the hydrophobic polymer surface at different pH values indicates a greater influence of the presence of hydroxide ions compared with protons; e.g., similar surface patterning is obtained at pH 1.5 and 11, even though the $[\text{H}_3\text{O}^+]$ in the former case is much larger than the $[\text{OH}^-]$ in the latter. This result suggests a preferential adsorption of OH^- with respect to H_3O^+ on the hydrophobic substrate. It has been reported many times that hydrophobic interfaces^{11–13} and even gas bubbles¹⁴ are negatively charged in contact with water at neutral or basic pH and become positively charged in acidic solutions. The origin of this charge is hotly debated.¹⁵ The main disagreement comes from the fact that the majority of experiments suggest a preferential adsorption of hydroxide ions, while the opposite picture has emerged from reports of surface sensitive spectroscopic techniques and MD simulations.^{15,16} Clearly, our results point in the direction of preferential OH^- adsorption.

2. Degassed solutions of most inorganic electrolytes evaluated did not induce large structuration on PS surfaces. Some examples are presented in Figure 2. With this kind of salts, the observed mild surface deformation is similar to the one obtained by treatment with degassed water at neutral pH. As a remarkable exception to this rule, relatively large bumps

Table 1. Structuring Effect of Different Salts at 0.03 M

	OH ⁻	Cl ⁻	Br ⁻	I ⁻	NO ₃ ⁻	ClO ₄ ⁻	SO ₄ ²⁻	CH ₃ COO ⁻	B(Ph) ₄ ⁻	C ₁₂ O ₂₅ SO ₄ ⁻
H ₃ O ⁺		✓			✓					
Li ⁺		X	✓	✓			X			
Na ⁺	✓	X	X	X	X	X		X	✓	✓
K ⁺	✓	X		X			X			
Cs ⁺				X						
NH ₄ ⁺		X			X					
Me ₄ N ⁺				✓						
Et ₄ N ⁺				✓						
Bu ₄ N ⁺		✓	✓	✓	✓					
(Ph) ₄ As ⁺		✓								

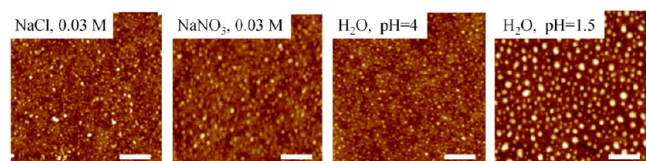


Figure 2. 1 $\mu\text{m} \times 1 \mu\text{m}$ height tapping mode AFM micrographs taken in air of 300 nm thick 250 kDa PS films treated with degassed water at different pHs (varied with HNO₃) or salt concentrations, as indicated. The scale bars correspond to 200 nm.

(although at a lesser density) are observed after treatment of PS surfaces with degassed solutions of some lithium salts (see below).

3. Degassed aqueous solutions of amphiphilic ions (e.g., sodium dodecyl sulfate, SDS, dodecyltrimethylammonium bromide, DTAB) or hydrophobic ions (e.g., halides of tetraalkylammonium quaternary, Figure 3; Ph₄BNa or Ph₄AsCl,

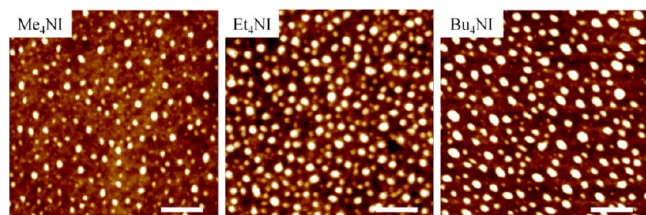


Figure 3. 1 $\mu\text{m} \times 1 \mu\text{m}$ height tapping mode AFM micrographs taken in air of 300 nm thick 250 kDa PS films treated with degassed 0.03 M solutions of different R₄NI salts (R = alkyl), as indicated. Bu = *n*-butyl; Et = ethyl; Me = methyl. More important surface deformation is observed for larger R (ethyl and *n*-butyl versus methyl). The scale bars correspond to 200 nm.

Figure 4) induce substantial deformation of the PS surfaces. The hydrophobicity of the ion seems to have a distinctive influence on the nanostructuration. As can be observed in

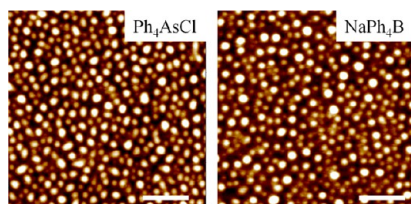


Figure 4. AFM micrographs of 300 nm thick PS films after 5 min exposure to 0.03 M degassed water solutions of tetraphenylarsonium chloride, Ph₄AsCl, and sodium tetraphenylborate, NaPh₄B. The scale bars correspond to 200 nm.

Figure 3, the longer is the chain length of tetraalkylammonium iodide salts the larger is the typical size of the induced nanostructure. Furthermore, ions with similar molecular structure seem to induce similar nanostructuration effect, regardless of the sign of the charge. For example, the salt Ph₄BNa induces the same effect as Ph₄AsCl (Figure 4), probably due to the similar effect of the tetraphenyl ions of opposite charge.

4. The observed nanostructuration is not just due to the effect of a particular ion, but to the combined influence of the different ions present in solution. As can be observed in Figure 5, the structuration effect of tetrabutylammonium salts is different for different counterions. The size of the bumps was larger for the case of iodide or bromide compared with nitrate or chloride. A more marked difference is observed for the case of lithium salts, as can be observed in Figure 6. While LiCl and LiSO₄ did not induce extensive surface structuration, substantial effect of LiI and LiBr solutions was observed. In addition, the degree of anionic induced structuration (quantified by size and density of self-assembled bumps) follows the anions' Hofmeister series.¹⁷ As a comparison, sodium or potassium salts with similar counterions did not produce any noticeable surface modification.

5. For salts that do not provoke extensive structuration of PS surfaces, there is no appreciable effect of salt concentration up to 0.1 M. This indicates that the small structuration observed in these cases (Figure 2) is mainly determined by the small amount of water ions present in the solutions. On the contrary, for salts with larger structuring influence, the resulting morphology depends on salt concentration. In general, higher concentrations result in higher surface charge density (vide infra) and in a more important modification of the polymer surface. Typically, the surface structuration was no longer enhanced for concentrations above 0.03 M. Some examples of the influence of salt concentration for structuring and nonstructuring ions in the IPN process are presented as Supporting Information.

B. Ions' Interaction with PS Surfaces: ζ . Our earlier results suggested that IPN is related to the interaction of ions with hydrophobic surfaces.² In this work, we performed complementary studies of the ionic influence on PS using ζ and surface interaction forces (by AFM) in the presence of different salts to confirm this scenario. Even though our experimental setups did not allow us to keep the aqueous solutions free of dissolved air, we think these results are of great help to improve our understanding of ionic solutions in contact with hydrophobic surfaces. In the IPN process the main effect of degassing is to increase the interaction between adsorbed ions and the polymer substrate by reducing their effective

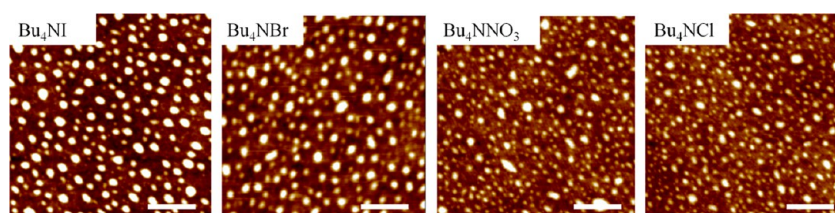


Figure 5. $1\ \mu\text{m} \times 1\ \mu\text{m}$ height tapping mode AFM micrographs of 300 nm thick PS films after 5 min exposure to 0.03 M degassed water solutions of different tetra-*n*-butylammonium salts. The scale bars correspond to 200 nm.

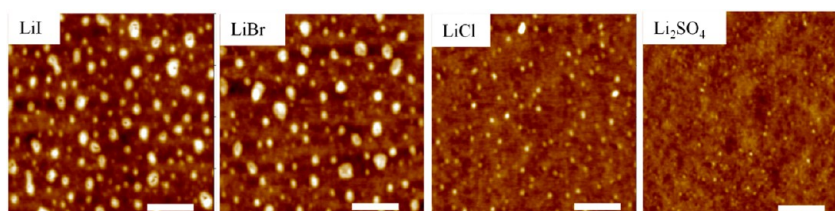


Figure 6. $1\ \mu\text{m} \times 1\ \mu\text{m}$ height tapping mode AFM micrographs of 300 nm thick PS films after 5 min exposure to 0.03 M degassed neutral water solutions of different lithium salts. The scale bars correspond to 200 nm.

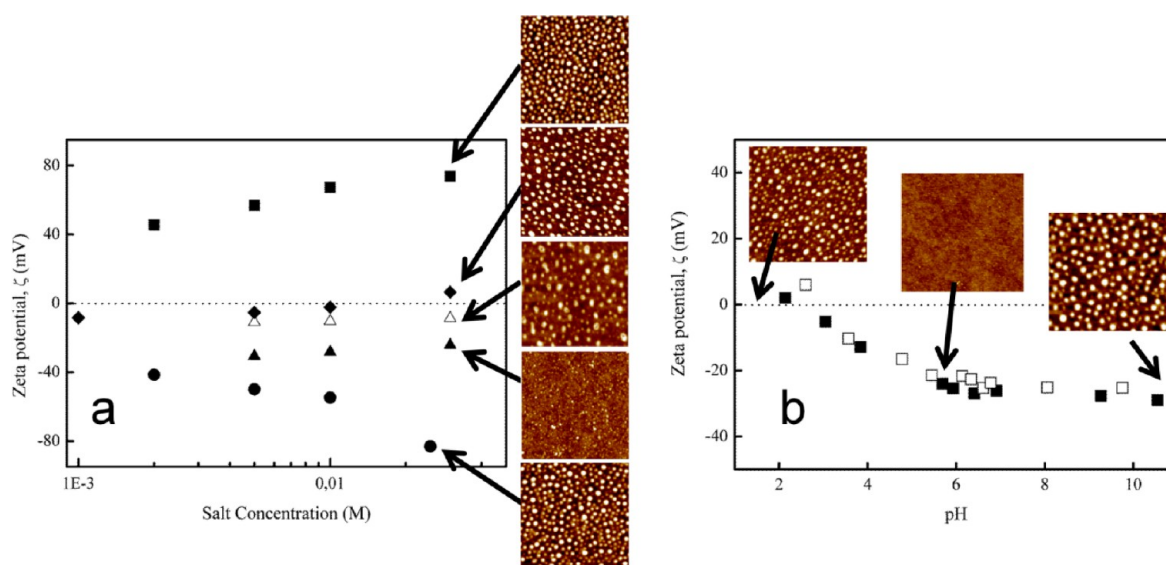


Figure 7. (a) ζ of PS films in the presence of selected salt solutions: squares, Ph_4AsCl ; circles, Ph_4BNA ; closed triangles, NaCl and KCl ; open triangles, LiI ; rhombi, Bu_4NI . A single salt was used on each test. (b) ζ of PS films (closed squares) and *n*-octadecyltrichlorosilane (OTS)-coated silicon wafers (open squares) as a function of pH. The pH was varied by addition of HCl or NaOH . Similar results were obtained with HNO_3 . The $1\ \mu\text{m} \times 1\ \mu\text{m}$ AFM micrographs show the corresponding surface morphology of PS films after IPN treatment.

separation; however, ionic adsorption is still observed in the presence of dissolved gases, as is shown below.

A compilation of some of our ζ results is presented in Figure 7. As can be observed in the figure, the ionic environment has a strong influence on ζ . Large ζ absolute values are observed at high or low pHs or in the presence of certain salts. The most significant effect was observed for strongly adsorbing tetraphenyl organic ions; an analogous variation of electrophoretic mobility of PS latexes in the presence of these salts has been recently reported by one of us.¹⁸ Charge reversal (with respect to the charge measured in pure water or in the presence of indifferent salts, e.g. NaCl) was observed in the presence of adsorbing cationic species (e.g., Bu_4NI or Ph_4AsCl) at sufficiently large concentrations. Interestingly, a good correlation is observed between the measured ζ variation (respect to the value measured in pure water) and IPN: the higher the salt-induced changes of ζ , the larger is the effect of the aqueous

phase on the polymer surface. This important result supports the idea of the electrohydrodynamic origin of IPN.²

Many hydrophobic polymers (e.g., PS) are inert as they do not have reactive surface groups. In addition, by virtue of their low dielectric constant they should not have a strong affinity for ions. However, it has been widely reported that they often exhibit electrokinetic potentials of the same order of charged hydrophilic surfaces (such as glass) and have similar pH dependence.¹⁵ In neutral or basic solutions they show a negative surface charge, which switch to positive values at pH below the isoelectric point (IEP), usually close to $\text{pH} = 4$. Similar results are typically found for hydrophobic surfaces of different nature. This behavior, which is also observed by us (Figure 7), supports the counterintuitive idea that hydrophobic surfaces can get charged due to specific ionic adsorption. However, it is important to emphasize here that ζ measures the

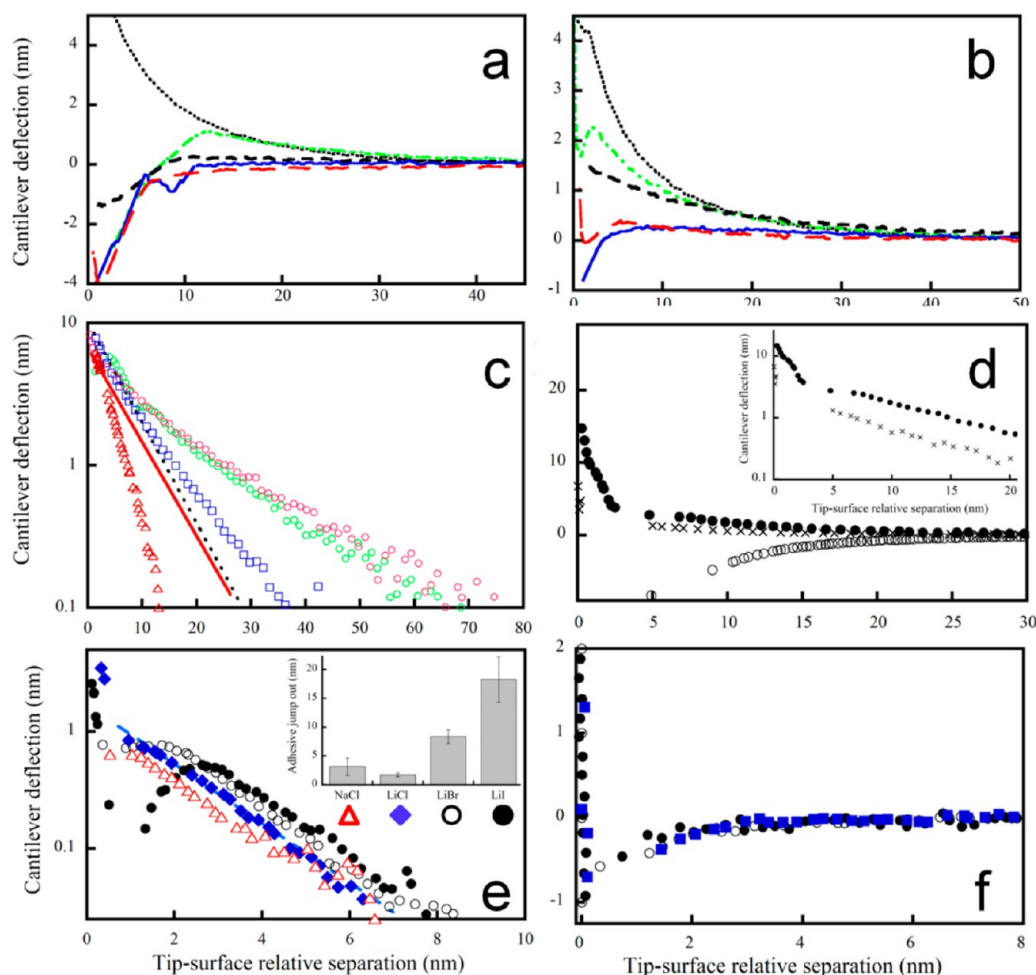


Figure 8. Normal interaction force measured by AFM between a silicon tip and (a) PS or (b) mica surfaces in water at different pH: pH 10.4 (dotted black line), 9.3 (dotted-dashed green line), 5.3 (short-dashed black line), 4.0 (continuous blue line), and 3.2 (long-dashed red line). (c–f) Normal interaction force measured by AFM between a silicon tip and a PS surface in water in the presence of (c) Ph_4BNA , after previous exposure to 10 mM of the same salt: Ph_4BNA concentration 0.1 mM (circles), 1 mM (squares), and 10 mM (triangles). Different colors correspond to different cycles, to illustrate reproducibility. The force profiles measured before exposure to 10 mM Ph_4BNA are shown by the continuous (1 mM) and dashed (0.1 mM) lines. (d) Closed circles, 1 mM Ph_4BNA ; open circles, 1 mM Ph_4AsCl ; crosses, 1 mM NaCl . Inset: same results in semilog representation. (e) 10 mM lithium halides: closed circles, LiI ; open circles, LiBr ; rhombi, LiCl . (NaCl , triangles, is shown as a reference.) The dashed line corresponds to an exponential-decay fit of the data measured for LiCl (see text). Inset: measured adhesive jump-out, averaged over 30 curves. (f) 10 mM Tetrabutylammonium halides: closed circles, But_4NI ; open circles, But_4NBr ; squares, But_4NCl .

amount of ions near the surface which does not necessarily correspond to the amount of tightly surface-bound ions.

The increasing (decreasing) ζ values at larger concentrations of particular cations (anions) strongly suggest that in most cases ionic adsorption is responsible for the surface charge (instead of a process of surface ionization due to the spurious presence of ionizable groups). Otherwise, the measured ζ should decrease with increasing ionic strength due to the compression of the electrical double layer, as is indeed observed for some salts, e.g., KCl . However, an alternative explanation can be advanced. As mentioned above, finite slip of the solvent at a charged surface considerably enhances the measured ζ . It has been proposed that for a nonzero slip length, b , the measured ζ is related to the surface potential Ψ by an amplification factor $(1 + b/\lambda_d)$, where λ_d is the Debye length characterizing the extension of the electrical double layer on the surface.⁹ Thus, as increasing salt concentration progressively reduces λ_d , the slip-induced amplification of ζ will be more important at larger ionic strengths. The ionic specificity observed argues against this explanation, if b is not ion-

dependent. However, we have not attempted to determine the particular value of b for each of the salts investigated. Instead, we have measured AFM force curves in liquid environment to complement our electrokinetic data and further investigate the influence of the ionic environment on the PS surface.

C. Influence of Ions on Tip–Substrate Interaction Forces Measured by AFM. We studied the interaction between silica probes and PS or mica substrates in the presence of different ions. Particularly, we investigated the effect of pH, the two tetraphenyl ions of opposite charge discussed above, and different lithium and tetrabutylammonium halides.

(i). *pH.* The effect of pH on the tip–substrate interaction for bare mica and PS-coated silicon wafers is presented in Figure 8. For the case of mica (Figure 8b), a long-range repulsive interaction is observed for all the pH values investigated. This result was expected, because mica and silica tips are both negatively charged at pH values above 3; it is well established that the electrostatic interaction between similarly charged surfaces is always repulsive (the opposite is not necessarily true; vide infra).¹⁹ The magnitude of the repulsive interaction

decreases substantially at low pH values due to the reduction of the surface charge density of the mica surface and the tip (the isoelectric point of silica is commonly found between pH = 2 and 3). At small tip–substrate separations the van der Waals (vdW) attraction dominates the interaction force. Similar results have been reported in the past.²⁰

A different scenario is observed for the case of PS surfaces (Figure 8a). Similarly to the case of mica, a long-range repulsive force of electrostatic origin dominated by the vdW attractive force at shorter separations is observed for pH values above 5. However, this repulsion quickly decreases at lower pH values. For pH = 4 or lower no signal of repulsive interaction is observed: instead, a long-range attractive force is measured. As mentioned above, the electrostatic interaction between similarly charged surfaces is always repulsive. The transit from repulsive to attractive electrostatic interaction is an unequivocal sign of surface charge reversal, in agreement with the ζ data. The interaction force measured at pH = 4 is quite revealing. Even though an attractive force is observed at large separations, an inflection point in the force profile is observed; for D between 10 and 7 nm the interaction becomes decreasingly attractive (more repulsive) before being overcome by the attractive vdW interaction for $D < 5$ nm. To bring to light this nonmonotonic behavior, the result presented in Figure 8a corresponds to a single profile (nonaveraged). A crossover from attractive to repulsive electrostatic interaction between oppositely charged surfaces has been predicted to be possible in the range $D < \text{ca. } 10$ nm for asymmetric surfaces²¹ (surfaces with different absolute values of charge density) but has never been observed before. This regime is difficult to detect because the repulsive interaction is promptly overcome by the attractive vdW interaction in this range of surface separations.²²

(ii). *Ph₄BNa versus Ph₄AsCl Salts*. Figure 8c,d shows the interaction force between the AFM tip and a PS surface in the presence of Ph₄BNa or Ph₄AsCl at different concentrations. The substrates were exposed to cycles of increasing salt concentrations, alternated with extensive water rinsing. Our AFM results evidence that the high values of ζ measured in the presence of these hydrophobic ions are due to ionic adsorption and not to ionization of charged groups.

As can be observed in Figure 8c, the tip–PS interaction force measured in the presence of Ph₄BNa was always repulsive and decayed exponentially with the relative tip–surface separation. However, when the PS surface was exposed to low salt concentrations for the first time ($<10^{-3}$ M), the decay length was seemingly independent of salt concentration, and shorter than the expected Debye length. This result can be understood as the interaction between a surface of small charge density and a charged tip of radii smaller than the Debye length, as described by Butt.²³ On the contrary, after the PS substrate is exposed once to larger Ph₄BNa concentrations (i.e., 10 mM), the decay of the force curves is well described by the theoretically expected Debye length even at low salt concentration (0.1 mM). These results corroborate the electrostatic origin of the repulsive force and indicate that the adsorption of Ph₄B on the PS substrate was at least partially irreversible. Strong affinity of this ion for hydrophobic surfaces driven by hydrophobic interaction has been recently reported, in agreement with our results.¹⁸

Figure 8d shows tip–PS AFM force curves measured in the presence of 1 mM Ph₄BNa or Ph₄AsCl. It is clear that the charge of the PS substrate depends on the ionic environment. As mentioned before, the PS surface becomes strongly

negatively charged in the presence of Ph₄BNa; the opposite is true for the case of Ph₄AsCl, consistent with our ζ data. A much smaller repulsive force is observed in the presence of NaCl (which is also shown for comparison). A different scenario is observed with hydrophilic mica surfaces (results not shown): the interaction is repulsive for all the salts, due to the negative surface charge of mica and tip.²³

(iii). *Lithium Salts*. An anomalous behavior of Li⁺ interacting with hydrophobic surfaces has been reported in the past. Li⁺ exhibits salting-out capabilities less marked than expected from its small size. It stabilizes protein secondary structures²⁴ or promotes surfactant micellar formation less effectively than Na⁺,²⁵ even though the opposite could be expected from its smaller size. Creux et al. observed a greater adsorption of Li⁺ at the air–water interface than other alkali ions.²⁶ Klasczyk²⁷ et al. reported a stronger affinity of Li⁺ for POPC vesicles than other ions in the alkaline group. These effects have often been attributed to the strong hydration of Li⁺.²⁵ Specific interaction between Li and certain function groups has also been evoked.²⁸

As shown in Figure 7, we have observed a less negative ζ for PS surfaces in contact with lithium halides compared with sodium or potassium counterparts. However, we are not able to discriminate between the different lithium salts which, as shown before, produced different IPN patterns. To further investigate this point, we measured AFM force curves with PS surfaces in the presence of 10 mM of different lithium salts. As can be observed in Figure 8e, a repulsive exponentially decaying profile with a similar decay length was observed for all the salts investigated. However, the characteristic length of the repulsion decay (1.7 nm) is shorter than the Debye length expected from the Gouy–Chapman theory for the salt concentration investigated (3.0 nm). As a comparison, the decay length measured for the interaction with a mica substrate (for the same salt solutions, with the same tip) was very close to what could be expected from the theory. As mentioned above, the reduced decay length suggests that the charge on the PS substrate is not large; thus, we are measuring the interaction between a charged object (the tip) and a surface with a small charge density.²³ As shown by Parsegian and Gingell,¹⁹ the interaction force between dissimilar objects with charge densities σ_1 and σ_2 is proportional to $(\sigma_1^2 + \sigma_2^2)e^{-2\kappa x} + (\sigma_1 + \sigma_2)e^{-\kappa x}$, where κ^{-1} is the Debye length. If $\sigma_1 \ll \sigma_2$, the first term of this expression will prevail and the observed decay length of the interaction force will be half of the Debye length. As can be observed in Figure 8e, the force profiles measured in the presence of the different lithium halides are not identical. However, the quantitative comparison between the different curves needs to be handled with care: as mentioned in the experimental section, the absolute tip–substrate separation is not known. The choice of the origin of the distance axes is somehow arbitrary, and it may not correspond to the actual tip–substrate contact in all cases. As a consequence of the exponential decay of the interaction force, a small shift in separation results in a large shift of interaction force. However, our results do not seem to suggest Li adsorption on the PS substrates. As a comparison, the effect on the tip–PS interaction of a truly adsorbing cation is illustrated in Figure 8f. In the presence of 10 mM tetrabutylammonium halides, an attractive tip–PS interaction is clearly observed. As discussed above, this can only mean that the charge of the PS surfaces has been reversed—compared with the small negative charge measured in pure water—due to ionic adsorption, in agreement with the streaming potential results.

How can the effect of Li salts be understood? It is interesting to consider the retraction part of the force curves. While strong adhesion and large jump outs are observed in the case of LiI and LiBr, the opposite is true for LiCl and NaCl (inset of Figure 8e). This suggests that the actual tip–substrate separation under high normal forces was smaller for the first two salts, which is probably an indication of diminished repulsive hydration forces. It is tempting to identify this reduction with the enhanced IPN observed. The reduced hydration repulsion would be due to strongly hydrated Li^+ ions competing for water molecules with the hydrophobic substrate. This facilitates the adsorption of large polarizable ions (e.g., I^-), which are then directly responsible for the enhanced IPN. This would explain why no IPN was observed in the presence of iodide of other, less hydrated, alkaline cations (e.g., Cs^+) or of lithium salts with less polarizable anions (e.g., Cl^-). However, clear conclusions cannot be drawn, given that we are measuring the interaction between asymmetric surfaces (SiO_2 tip and PS) with dissimilar effects on the neighboring water. Although hydration forces has been discussed and reported for many years,^{29–31} the actual mechanism behind this short-range interaction force and the reason for ionic specificity are matters of active research. In addition, it is conceivable that the presence of the AFM tip perturbs the ionic distribution around the PS surface. It is also possible that degassing enhances the dispersive interaction between ions and PS substrate, improving adsorption of polarizable ions. Hence, failing to keep degassed conditions makes it difficult to point out the distinctive effect of different Li and tetrabutylammonium halides. In any case, our results show that it is not enough to consider the behavior of specific ions in studies of ionic adsorption: an adequate description of the problem must include the combined influence of all the species present in solution. These results also suggest that the structuring influence of lithium salts is the result of a subtle combination of effects controlling the ionic environment around hydrophobic PS surfaces.

From the different experimental results presented in this work, it seems apparent that the IPN process is governed by ionic adsorption on the hydrophobic polymer surface. It is then important to understand what determines this adsorption in order to control the outcome of the process. It has been suggested that ionic specific adsorption can be described in terms of the “law of matching affinities” proposed by Collins.³² Following this rule, we could explain the adsorption of ions of large size and small density of charge (chaotropic ions, in Collins’ classification) if we consider the PS substrate as a “chaotropic” entity in the limit of very low charge density (the similar effect of oppositely charged ions precludes the idea of ion pair formation). However, under this framework it will be difficult to rationalize the well-established adsorption of water ions, which by no means can be considered as chaotropic. It will be also difficult to explain the distinctive behavior of different alkali halides or other seemingly similar ion pairs. On the contrary, the combination of hydrophobic interaction, dispersion forces, and the surface dewatering effect of strongly hydrated ions may provide a full account of our observations.

CONCLUSIONS

Ion adsorption induces a long-lasting deformation of the surface of hydrophobic glassy PS films. This process is highly ion specific, and is favored by larger ionic concentrations for ions with a favorable interaction with the substrate. This phenomenon is likely to be relevant for many processes

involving the interface between water and hydrophobic objects. It should be particularly relevant for biological processes that involve large hydrophobic ions susceptible of getting adsorbed on hydrophobic substrates.

ASSOCIATED CONTENT

Supporting Information

Some examples of the influence of salt concentration on surface structuration are presented. This material is available free of charge via the Internet at <http://pubs.acs.org>.

AUTHOR INFORMATION

Corresponding Author

*Phone: +33-556845612. E-mail: drummond@crpp-bordeaux.cnrs.fr.

Present Address

[†]Physics of Complex Fluids, MESA Institute for Nanotechnology, University of Twente, Post Office Box 217, 7500 AE Enschede, The Netherlands.

Author Contributions

The manuscript was written through contributions of all authors. All authors have given approval to the final version of the manuscript.

Notes

The authors declare no competing financial interest.

ACKNOWLEDGMENTS

The financial support of the European Union and the MICINN, Spain (MAT 2012-3670-C04-02), the University of Granada (CEIBioTic 20F12/16), the Junta de Andalucía (CTS-6270 and IAC 2/2011), and the University of Bordeaux 1 (BQR 2009) is gratefully acknowledged.

REFERENCES

- (1) Robert, J. Hunter *Foundations of Colloid Science*, 2nd ed.; Oxford University Press: Oxford, UK, 2001.
- (2) Siretanu, I.; Chapel, J. P.; Drummond, C. Water-Ions Induced Nanostructuration of Hydrophobic Polymer Surfaces. *ACS Nano* **2011**, *5*, 2939–47.
- (3) Siretanu, I.; Chapel, J. P.; Drummond, C. Substrate Remote Control of Polymer Film Surface Mobility. *Macromolecules* **2012**, *45*, 1001–1005.
- (4) Butt, H.-J.; Cappella, B.; Kappl, M. Force Measurements With the Atomic Force Microscope: Technique, Interpretation and Applications. *Surf. Sci. Rep.* **2005**, *59*, 1–152.
- (5) Tyrrell, J. W. G.; Attard, P. Images of Nanobubbles on Hydrophobic Surfaces and Their Interactions. *Phys. Rev. Lett.* **2001**, *87*, 176104.
- (6) Ishida, N.; Inoue, T.; Miyahara, M.; Higashitani, K. Nano Bubbles on a Hydrophobic Surface in Water Observed by Tapping-Mode Atomic Force Microscopy. *Langmuir* **2000**, *16*, 6377–6380.
- (7) Joly, L.; Ybert, C.; Trizac, E.; Bocquet, L. Hydrodynamics within the Electric Double Layer on Slipping Surfaces. *Phys. Rev. Lett.* **2004**, *93*, 1–4.
- (8) Rossky, P. J. Exploring Nanoscale Hydrophobic Hydration. *Faraday Discuss.* **2010**, *146*, 113–124.
- (9) Bouzigues, C.; Tabeling, P.; Bocquet, L. Nanofluidics in the Debye Layer at Hydrophilic and Hydrophobic Surfaces. *Phys. Rev. Lett.* **2008**, *101*, 12–15.
- (10) Doshi, D. A.; Watkins, E. B.; Israelachvili, J. N.; Majewski, J. Reduced Water Density at Hydrophobic Surfaces: Effect of Dissolved Gases. *Proc. Natl. Acad. Sci. U.S.A.* **2005**, *102*, 9458–62.
- (11) Marinova, K. G.; Alargova, R. G.; Denkov, N. D.; Veleev, O. D.; Petsev, D. N.; Ivanov, I. B.; Borwankar, R. P. Charging of Oil–Water

Interfaces Due to Spontaneous Adsorption of Hydroxyl Ions. *Langmuir* **1996**, *12*, 2045–2051.

(12) Beattie, J. K.; Djerdjev, A. M. The Pristine Oil/Water Interface: Surfactant-Free Hydroxide-Charged Emulsions. *Angew. Chem., Int. Ed.* **2004**, *43*, 3568–71.

(13) Zimmermann, R.; Dukhin, S.; Werner, C. Electrokinetic Measurements Reveal Interfacial Charge at Polymer Films Caused by Simple Electrolyte Ions. *J. Phys. Chem. B* **2001**, *105*, 8544–8549.

(14) Yang, C.; Dabros, T.; Li, D.; Czarnecki, J.; Masliyah, J. H. Measurement of the Zeta Potential of Gas Bubbles in Aqueous Solutions by Microelectrophoresis Method. *J. Colloid Interface Sci.* **2001**, *243*, 128–135.

(15) Zimmermann, R.; Freudenberger, U.; Schweiß, R.; Küttner, D.; Werner, C. Hydroxide and Hydronium Ion Adsorption — A Survey. *Curr. Opin. Colloid Interface Sci.* **2010**, *15*, 196–202.

(16) Jungwirth, P.; Winter, B. Ions at Aqueous Interfaces: From Water Surface to Hydrated Proteins. *Annu. Rev. Phys. Chem.* **2008**, *59*, 343–66.

(17) Kunz, W. Specific Ion Effects in Colloidal and Biological Systems. *Curr. Opin. Colloid Interface Sci.* **2010**, *15*, 34–39.

(18) Calero, C.; Faraudo, J.; Bastos-González, D. Interaction of Monovalent Ions with Hydrophobic and Hydrophilic Colloids: Charge Inversion and Ionic Specificity. *J. Am. Chem. Soc.* **2011**, *133*, 15025–35.

(19) Parsegian, V. a; Gingell, D. On the Electrostatic Interaction across a Salt Solution between Two Bodies Bearing Unequal Charges. *Biophys. J.* **1972**, *12*, 1192–204.

(20) Hartley, P. G.; Larson, I.; Scales, P. J. Electrokinetic and Direct Force Measurements between Silica and Mica Surfaces in Dilute Electrolyte Solutions. *Langmuir* **1997**, *13*, 2207–2214.

(21) Ben-Yaakov, D.; Burak, Y.; Andelman, D.; Safran, S. a Electrostatic Interactions of Asymmetrically Charged Membranes. *Europhys. Lett.* **2007**, *79*, 48002.

(22) Kampf, N.; Ben-Yaakov, D.; Andelman, D.; Safran, S. a.; Klein, J. Direct Measurement of Sub-Debye-Length Attraction between Oppositely Charged Surfaces. *Phys. Rev. Lett.* **2009**, *103*, 118304.

(23) Butt, H.-J. Electrostatic Interaction in Atomic Force Microscopy. *Biophys. J.* **1991**, *60*, 777–785.

(24) Borén, K.; Grankvist, H.; Hammarström, P.; Carlsson, U. Reshaping the Folding Energy Landscape by Chloride Salt: Impact on Molten-Globule Formation and Aggregation Behavior of Carbonic Anhydrase. *FEBS Lett.* **2004**, *566*, 95–9.

(25) Carale, T. R.; Pham, Q. T.; Blankschtein, D. Salt Effects on Intramolecular Interactions and Micellization of Nonionic Surfactants in Aqueous Solutions. *Langmuir* **1994**, *10*, 109–121.

(26) Creux, P.; Lachaise, J.; Graciaa, A.; Beattie, J. K. Specific Cation Effects at the Hydroxide-Charged Air/Water Interface. *J. Phys. Chem. B* **2007**, *111*, 3753–3755.

(27) Klasczyk, B.; Knecht, V.; Lipowsky, R.; Dimova, R. Interactions of Alkali Metal Chlorides with Phosphatidylcholine Vesicles. *Langmuir* **2010**, *26*, 18951–8.

(28) Beauchamp, D. L.; Khajepour, M. The Effect of Lithium Ions on the Hydrophobic Effect: Does Lithium Affect Hydrophobicity Differently than Other Ions? *Biophys. Chem.* **2012**, *163–164*, 35–43.

(29) Pashley, R. M.; Israelachvili, J. N. DLVO and Hydration Forces between Mica Surfaces in Mg^{2+} , Ca^{2+} , Sr^{2+} , and Ba^{2+} Chloride Solutions. *J. Colloid Interface Sci.* **1984**, *97*, 446–455.

(30) Ben-Yaakov, D.; Andelman, D.; Podgornik, R.; Harries, D. Ion-Specific Hydration Effects: Extending the Poisson-Boltzmann Theory. *Curr. Opin. Colloid Interface Sci.* **2011**, *16*, 542–550.

(31) Chapel, J.-P. Electrolyte Species Dependent Hydration Forces between Silica Surfaces. *Langmuir* **1994**, *10*, 4237–4243.

(32) Collins, K. D. Why Continuum Electrostatics Theories Cannot Explain Biological Structure, Polyelectrolytes or Ionic Strength Effects in Ion-Protein Interactions. *Biophys. Chem.* **2012**, *167*, 43–59.